Article:
Liu, S, Wang, J, Yu, HS orcid.org/0000-0003-3330-1531 et al. (3 more authors) (2022) Shakedown of asphalt pavements considering temperature effect. The International Journal of Pavement Engineering, 23 (5). pp. 1572-1583. ISSN 1029-8436

https://doi.org/10.1080/10298436.2020.1812068

Shakedown of asphalt pavements considering temperature effect

Shakedown limit has been perceived as a useful guidance in pavement structure design against rutting. However, temperature, as one of the most important factors influencing the shakedown limit of asphalt pavements, has barely been considered in previous studies. In this paper, the shakedown phenomenon was first identified from wheel tracking tests for a pavement structure consisting of a dense bituminous macadam (DBM) layer and a granular layer in a temperature-controlled condition. The friction angles, cohesion and stiffness moduli of the granular material and the DBM at the same temperature (40°C) were obtained using a series of tests. Based on a previously developed shakedown approach and the material properties, lower-bound shakedown limits of the layered system were determined and compared with the wheel tracking test results. Following that, an empirical relation between temperature and cohesion of asphalt mixture was suggested. A temperature-dependent shakedown approach was then proposed which can quickly obtain the shakedown limits of asphalt pavements over a range of temperatures. Results show that the shakedown limits decrease markedly with increasing temperature, accompanied by a shift of the failure mode from a granular layer failure to an asphaltic layer failure. It is also found that the most effective and economic way to enhance the pavement performance under high temperature is improving shear strength properties of asphalt mixtures rather than increasing asphalt layer thicknesses. By using this method, pavement stability against rutting can be evaluated efficiently at any temperature.

Keywords: asphalt pavements; wheel tracking test; temperature; shakedown; cohesion

Introduction

An elastic-plastic structure subjected to cyclic or repeated loads could respond in a resilient manner when the load applied is above the yield limit but lower than a critical load limit. This phenomenon is known as shakedown and the load limit is termed as the shakedown limit. Otherwise, a larger load may lead to a continuous accumulation of permanent deformation (Yu 2006). In pavement engineering, shakedown theory is useful for design against pavement failure in the form of excessive rutting.

The shakedown behaviour of granular materials and soils has been widely studied through laboratory tests. For example, Lekarp et al. (1996) conducted repeated triaxial tests on five different aggregates and pointed out that there is a threshold stress ratio under which a shakedown behaviour could be observed. A number of cyclic triaxial tests were also reported by Wellner and Werkmester (2000) and Werkmeister (2005) for granodiorite and sandy gravel. The results were illustrated by plotting cumulative vertical permanent strain against vertical permanent strain rate. Shakedown was recognised when the accumulated plastic strain rate per cycle became very small. European Standard (BS EN 13286-7:8, 2004) suggested that in a cyclic triaxial test, a shakedown status can be identified if the difference between plastic strains at 3000 and 5000 load cycles is smaller than 0.045×10^{-3}. Considering a more realistic heart-shape stress path due to a moving load, cyclic hollow cylinder tests on clay were conducted by Qian et al. (2016) and the energy dissipation trend was suggested as an indicator to distinguish shakedown and non-shakedown status. A series of wheel tracking tests were also reported in Juspi (2007) and Brown et al. (2012) using four types of soil and granular materials. Possible ranges of the shakedown limits for several single or layered systems were obtained.

For asphalt pavements, the shakedown phenomena was first identified in the mid-1980's (Sharp and Booker, 1984; Sharp 1985; Brett 1987) through analysing data from

the AASHO road tests and several road sections in New South Wales, Australia. Allou et al. (2010) reported the rutting test data of a full-scale pavement experiment in Nantes, France, consisting of an asphalt concrete layer, an unbound granular layer and subgrade soil. During around 2 million load applications, shakedown status was demonstrated as rutting gradually became stable. In laboratory tests, dense asphalt mixtures also exhibit shakedown behavior when the applied stress level is low (Fwa et al. 2004, Wasage et al. 2010, Ahmad et al. 2011, Wang 2015). For example, in the cyclic triaxial tests of a dense asphalt mixture, Wang (2015) found no obvious change in dissipated energy per cycle during the test when the stress ratio is below a certain value, which was considered as a shakedown limit. Despite those interesting observations, limited attention was paid to the origin of the distinct values of shakedown limits for different experimental situations, which should depend on material properties, loading conditions and pavement layout. A sound approach considering those key aspects is significant in the application of shakedown theory in asphalt pavement design.

Finite element simulations were considered as one obvious option. Assuming no plastic deformation occurs in the asphalt layer, Chazallon et al. (2009) incorporated a shakedown-based permanent deformation model for granular materials with finite element analysis to estimate the rutting depth of a pavement. Wang and Yu (2013a) and Liu et el. (2016) simulated the shakedown and non-shakedown behaviour of cohesive-frictional materials under moving surface loads of different magnitudes, but a significant computation effort was involved in order to identify the shakedown limit.

Compared with the numerical step-by-step simulations, theoretical shakedown analyses show a clear advance in that the shakedown limit can be determined in a direct manner without calculating the full stress-strain history. The theoretical shakedown analyses were conducted based on either Melan's static shakedown theorem (Melan

1938) or Koiter's kinematic shakedown theorem (Koiter 1960), which gives lower or upper bound to the actual shakedown limit. Various theoretical shakedown approaches for shakedown limits were developed for two-dimensional (2D) situations (e.g. Collins and Cliffe 1987, Raad et al. 1988, Boulbibane and Ponter 2005, Chen and Ponter 2005, Nguyen 2007, Krabbenhøft et al. 2007, Zhao et al. 2008) and three-dimensional (3D) situations (Yu and Wang 2012, Wang and Yu 2014, Liu et al. 2016, Wang et al. 2018). These shakedown solutions were solved based on different constraint conditions or mathematical optimisation methods for granular roads. More details can be found in Wang et al. (2018). In term of flexible pavements, the 3D shakedown approach of Yu and Wang (2012) has been applied for the design against rutting considering the effects of layer thickness and the elastic and plastic properties of materials. However, little effort was made on the evaluation of the effect of temperature on the shakedown limit. Although some two-dimensional shakedown limits were obtained by Boulbibane et al. (2000) considering several temperatures ranging from -15°C to 35°C, the rutting failure of asphaltic pavements is more relevant to material properties at high temperature (≥ 40°C). Moreover, there is still a lack of direct comparison between the theoretical shakedown solutions and experimental shakedown limits for asphalt pavements. Although some two-dimensional shakedown limits were obtained by Boulbibane et al. (2000) considering several temperatures from -15°C to 35°C, the rutting failure of asphaltic pavements is more relevant to material properties at high temperature (≥ 40°C). Moreover, there is still a lack of direct comparison between the theoretical shakedown solutions and experimental shakedown limits for asphalt pavements.

In this paper, shakedown and non-shakedown phenomena of a two-layered pavement system, made of an asphaltic layer and an unbound granular layer, are identified through wheel tracking tests in a temperature-controlled condition. After a series of

laboratory tests on the properties of the asphalt mixture and the unbound granular materials, the theoretical shakedown solutions for the pavement system are calculated and compared with the results from the wheel tracking tests. Following that, a temperature-dependent shakedown approach is proposed, which can be used to quickly evaluate the influence of temperature on the shakedown limit of an asphalt pavement.

Experimental identification of shakedown behavior in an asphalt pavement system

In the present study, wheel tracking tests (Figure 1) were performed in a temperature-controlled room at 40 °C. The surface load was applied by a solid rubber wheel (radius = 100 mm) mounted between a pair of beams. During the test, the wheel position was fixed. The motor-driven shaft spun anti-clockwise to drive the reciprocating table forward and backward at an average speed of 0.98 km/hr. A metal mould filled with a two-layered specimen was mounted on the reciprocating table. The wheel loads were applied by adding weights on the load hanger. Dimensions of the contact patches were measured under different load magnitudes by replacing the mounted mould with a digital scale covered by a piece of white paper. Several rigid slabs were laid under the digital scale to ensure that the top surface of the scale was the same height as the specimen surface. The wheel was smeared with black powder so that a print patch can be obtained on the white paper when adding weights on the hanger. It was found the shapes of the patches were more like rectangles, of which the dimensions were measured by a ruler. The contact pressure then can be calculated through dividing the weight by the contact area (Table 1). A Linear Variable Differential Transformer (LVDT) was fastened in a movable holder (Figure 2) to measure the rutting depth at the central point on the surface of the sample.

A two-layered specimen containing an asphaltic layer and an unbound granular layer was selected (Figure 3). The thicknesses of the two layers were chosen to be 25 mm and 75 mm, so that the ratios of the layer thicknesses to the length of contact area are close to realistic situations. Well-graded crushed granite with a maximum particle size of 2.8 mm was employed in the base layer, the gradation curve of which is shown in Figure 4. A total of 13.15 kg of crushed granite was divided into four equal parts and compacted into the metal mould layer by layer. A thin slab of dense bituminous macadam (DBM) comprising 82.1% by volume of broadly graded aggregate, 10.6% bitumen binder (50 Pen) and 7.3% voids was used as the top layer. The gradation curve of the asphalt aggregate is also given in Figure 4, which lies within the upper bound and lower bound suggested by British standard BS EN 12697-28 (2001) for high-quality asphalt mixtures.

Figure 5 presents the rutting depth along with the number of load passes under different surface pressures. Each test lasted several days since a very large number of load repetitions was applied. As no test could be carried out in the laboratory at night, the specimen was stored overnight at a temperature of 40°C. For the specimen subjected to 360 kPa surface pressure, an identical number of 8000 load passes was applied each day to investigate the effect of the overnight storage. It was found that the recovered deformation caused by the visco-elasticity of the asphalt was within 3% of the total permanent deformation. It is commonly known that most of the recoverable strains could be restored within a few hundred seconds. For instance, Bai et al. (2014) conducted creep-recovery tests for asphalt mixtures at a temperature of 20±2 °C and suggested a recovery duration ranging between 500 and 1700 seconds dependent on the stress level considered. Similar findings have also been reported by Chen et al. (2015) when considering asphalt mixtures with or without ground waste tyre fines at a temperature of 60 °C. In this study, since the overnight storage period was more than 8 hours, it is believed that most of the

recoverable deformation has been restored during the storage period. Therefore, the viscoelasticity of the asphalt mixture has a limited effect on the rutting depth in our study.

Considering the trend of the stress-strain curves, previous researchers have proposed various criteria to distinguish different behaviors of materials under cyclic loads. The behaviors were generally divided into three different categories, termed as Range A (shakedown status), Range B (plastic creep) and Range C (incremental collapse) respectively. It was suggested by Dawson and Wellner (1999) that if the permanent strain rate per load cycle decreases until the response becomes entirely resilient and the permanent strain rate quickly decreases to a very small level, the structure could be considered as being in a shakedown state (i.e. Range A). As can be seen in Figure 5, when the load level was relatively small (i.e. 296 kPa), the rutting depth barely changed after 40000 load passes; and the curve demonstrated a distinct trend that its tangent slope becomes shallower. Moreover, Figure 6 demonstrates the strain rate was very small below the magnitude of 6×10^{-7} or even slightly negative. The negative strain rate could be induced by the overnight storage or measurement errors. Therefore, the asphalt pavement under this load was in a shakedown state (Range A). When the load was 494 kPa or 560 kPa, the permanent deformation grew continuously with increasing number of load passes, and therefore the structure was in an obvious non-shakedown state, which can be defined as Range C (incremental collapse). When the load was at an intermediate level (i.e. 360 kPa or 444 kPa), the pavement behavior fell into Range B, where the permanent strain continuously developed after a large number of load passes, but the permanent strain rate tended to be constant (Figure 6). As a result, it can be inferred that the shakedown limit of this asphalt pavement system is between 296 kPa and 360 kPa. In pavement design, Range A is highly recommended, whereas Range C should be avoided

as much as possible. Range B is still acceptable if the rutting depth can be controlled within a sustainable value during the service life.

Comparison between theoretical and experimental results

Lower-bound shakedown approach

The theoretical shakedown approach for pavements adopted in the present study was first proposed by Yu and Wang (2012) and Wang and Yu (2013b) based on the static shakedown theorem of Melan (1983). The static shakedown theorem states that an elastic-plastic structure under cyclic or variable loads will shakedown if a self-equilibrated residual stress field σ_{ij}^{r} exists such that its superposition with the load-induced elastic stress field σ_{ij}^{e} does not exceed the yield criterion anywhere in the structure. This can be expressed as Eq. 1, where λ is a load factor. In the theoretical lower-bound shakedown approach for pavements, two critical residual stress fields σ_{xx}^{r} were derived. By substituting either of the critical residual stress fields, the unit load-induced elastic stress fields, and the Mohr-Coulomb criterion into Eq. 1, the problem becomes a unified mathematical optimisation problem as shown in Eq. 2, where f represents the Mohr-Coulomb yield function; c^{n} and ϕ^{n} are the cohesion and friction angle of the material at the n^{th} layer. σ^{e} represents the elastic stress field induced by a unit load P. The critical residual stresses σ_{xx}^{r} at any depth $z = j$ are functions of M and N, which also depend on the elastic stresses at every point i and the load factor. Their values at any depth $z = j$ can be calculated by searching for the minimum value of $-M_i + \sqrt{-N_i}$ or the maximum value of $-M_{\mathrm{i}} - \sqrt{-N_i}$ among all points. For each layer, the maximum admissible load factor is the shakedown limit of the layer, denoted as $\lambda_{\mathrm{sd}}^{n} P$. Finally, the shakedown limit of the

whole pavement structure is the minimum among the layer shakedown limits, as shown in Eq. 3. To calculate the theoretical shakedown limit for the experimental case, material property parameters required in Eq. 2 were determined through a series of laboratory tests. A flow chart is given in Figure 7 to demonstrate the main process.

$$f(\lambda\sigma_{ij}^{e}+\sigma_{ij}^{r})\le 0 \tag{1}$$

$$\max \lambda^{n},\quad s.t.\begin{cases} f(\sigma_{xx}^{r}(\lambda^{n}\sigma^{e}),\lambda^{n}\sigma^{e})\le 0 \text{ for each point } i \text{ in the n}^{\text{th}} \text{ layer},\\ \sigma_{xx}^{r}(\lambda^{n}\sigma^{e})=\min\limits_{z=j}(-M_i+\sqrt{-N_i}) \text{ or } \sigma_{xx}^{r}(\lambda^{n}\sigma^{e})=\max\limits_{z=j}(-M_i-\sqrt{-N_i}),\\ M=\lambda^{n}\sigma_{xx}^{e}-\lambda^{n}\sigma_{zz}^{e}+2\tan\phi^{n}(c^{n}-\lambda^{n}\sigma_{zz}^{e}\tan\phi^{n}),\\ N=4(1+\tan^{2}\phi^{n})[(\lambda^{n}\sigma_{xz}^{e})^{2}-(c^{n}-\lambda^{n}\sigma_{zz}^{e}\tan\phi^{n})^{2}] \end{cases} \tag{2}$$

$$\lambda_{sd}P=\min\{\lambda_{sd}^{1}P,\lambda_{sd}^{2}P,\ldots\lambda_{sd}^{\mathrm{n}}P\}. \tag{3}$$

Similar to the analytical pavement design method in the UK, the analysis here involves the usage of materials which are not perfectly linear-elastic, but an elastic stiffness modulus is used to reflect the response of the material to the wheel load. Moreover, it is considered that asphalt mixtures in the analysis have very good internal structures. This means at relatively high temperatures, the effect of the properties of the aggregates and aggregate interlock becomes more significant and the binder influence drops. Also, the viscoelastic deformation of asphalt mixtures is small under a specific range of design loads and loading frequencies. Therefore, the viscoelastic effects have been considered negligible.This is a limitation of the present research. The plastic behaviour of the materials is described by the Mohr-Coulomb model. The properties of granular materials (crushed granite) in the test were determined using consolidated drained triaxial tests under dry and fully-saturated conditions, respectively. The triaxial specimens were 50 mm in diameter and 100 mm in height and the relative density was

around 0.91. The general set-up of the triaxial cell is described in Rees (2013). Following previous works (Seed et al. 1954, Juspi 2007, Svoboda 2014), the loading rate was set as 1%/min for dry materials and 0.1 %/min for fully-saturated materials. The stress-strain curves are given in Figure 8.

According to Lambe and Whitman (2008), the stiffness moduli of granular materials under different confining pressures can be estimated from the slope of the line connecting the origin and the point corresponding to one-half of the peak deviator stress. Figure 9 demonstrates a linear relationship between the stiffness modulus and the confining pressure. This agrees with the findings of Kohata et al. (1997). In this study, the stiffness moduli under unconfined conditions (18.3 MPa for dry sample and 11.1MPa for saturated sample) were selected for the theoretical calculation. Plastic parameters were determined by plotting Mohr circles using the peak deviator stresses. A matching method proposed by Chen et al. (2009) was adopted to seek the failure lines. According to Figure 10, the friction angle and cohesion of the dry crushed granite are 50.9° and 45.6 kPa respectively. For the fully saturated materials, these values are 46.1° and 68.1 kPa respectively.

Properties of asphalt mixture

Tests on the asphalt mixture were conducted under a temperature of 40. An Instron 1332 loading frame (Figure 11) with a temperature-controlled cabinet and a servo-hydraulic actuator (load capacity = ± 100 kN, maximum axial stroke = ± 50 mm) was used. A triaxial chamber with a confining pressure capacity of 1.7 MPa was mounted inside the Instron universal tester cabinet. The cell pressure was controlled by an air pressure gauge attached to the triaxial chamber. Cylindrical asphalt specimens, 100 mm in diameter and 110 mm in height, were prepared and sealed with membranes. The temperature of the

cabinet was adjusted to 40°C and left overnight for preheating. During the test, the axial pressure was applied by lifting the base pedestal gradually at a rate of 1 mm/min until the peak axial load was reached. The tests were carried out under confining pressures of 50 kPa, 150 kPa and 200 kPa. Figure 12 demonstrates that the friction angle and cohesion of the asphalt were 34.1° and 315.1 kPa respectively.

The stiffness modulus of the asphalt mixture was determined using axial dynamic compression tests (ADCT) under a strain control condition. Considering different contact lengths and wheel moving speeds in the wheel tracking tests, the loading frequency was estimated to be 5~10Hz, and a frequency of 10 Hz was selected for this study. Further studies revealed that though the frequency has an obvious effect on the stiffness modulus of the asphalt mixture, its influence on the shakedown limit of the overall structure is small, because the relationship between layer stiffness and shakedown limit is nonlinear, as demonstrated in Wang and Yu (2013b). Figure 13 shows that the stiffness modulus became almost constant after a number of load cycles. Therefore, the stiffness modulus was taken as the slope of the secant connecting the zenith and the nadir of the last cycle (shown as the red line in Figure 13). The test was carried out twice and an averaged value, 891.8MPa, was taken finally. Table 2 summarises the material properties for the crushed granite and the asphalt mixture.

It should be noted that the permanent deformation of asphalt mixture is controlled by both the internal structure of aggregate skeletons and the viscous behavior of bitumen (Li et al. 2018). For an asphalt mixture with a good skeleton, the permanent deformation was largely affected by the interlocking of aggregate particles. However, in the case of a less good skeleton, such as Hot Rolled Asphalt, the viscous behavior of bitumen would dominate the permanent deformation, and therefore the shakedown theory is no longer applicable.

Comparison

Shakedown analyses were carried out considering a three-dimensional (3D) loading situation. The elastic stress fields were obtained by Finite Element (FE) analyses using ABAQUS. The 3D model was similar to that in Wang and Yu (2013b) which simulated one half of the pavement system, but a rectangular contact area was used instead. Sensitivity studies were conducted to obtain results of reasonable accuracy. Finally, a 3D model with 86060 C3D20R elements was used. For the mesh directly under the contact area, very small elements of size 1.7 mm (length) × 1.67mm (width) × 1.25mm (depth) were applied. The mesh gradually became coarser farther away from the contact area. The material parameters and layer thickness were used in the analysis. A typical value of 0.3 was selected as the Poisson ratio for both materials. There was an elastic steel layer (E = 206 GPa, $\nu = 0.31$) under these two layers, which represents the steel mould in the test. The surface pressure (P) was distributed uniformly over the rectangular contact area. Although the length of the contact area changes linearly with the load magnitude, its influence on the pavement shakedown limit was found to be very small. A contact length of 0.032 m was selected for all the simulations in Table 3. The contact width was equal to the width of the wheel (i.e. 0.05m). The horizontal surface traction was assumed to be correlated with the vertical pressure by a frictional coefficient μ, which however is difficult to be measured accurately. The frictional coefficient for a wheel moving at a constant speed is typically between 0.1 and 0.3, but the alternative acceleration and deceleration of the moving wheel in a short periodic time could result in a larger frictional coefficient. Therefore, various frictional coefficients were selected in the analysis. In Table 3, Cases 1 to 3 considered the dry crushed granite, while Cases 4 to 6 assumed a fully-saturated condition for the crushed granite. It is found the shakedown limits exceed the experimental shakedown range (i.e. 296 kPa to 360 kPa) if a small/zero surface

traction is considered (Cases 1, 2, 4 and 5). If the frictional coefficient is 1 (Cases 3 and 6), the shakedown solutions fall within the experimental shakedown limit range.

It should be noted that the lower the loading frequency the lower the stiffness modulus of the asphalt mixture. For the case studied here, the stiffness modulus of the asphalt mixture under a 5 Hz cyclic load was found to be 811.6 MPa, which is 9% lower than that at 10 Hz; however, the corresponding shakedown limit is only increased slightly (e.g. from 601.1 kPa to 613.9 kPa for Case 4). This is because when the first layer is much stiffer than the lower layer, the shakedown limit tends to decrease with increasing stiffness ratio, as depicted in Wang and Yu (2013b); and the impact of the first layer stiffness on the elastic stress distribution gets smaller as the stiffness ratio increases further.

Shakedown analysis of asphalt pavements

A temperature-dependent shakedown approach

Although design of asphalt pavement is usually conducted considering a moderate temperature (e.g. 20°C in the UK), pavement surface temperature could easily reach 60°C (Hofstra and Klopm 1972). A shakedown approach would become very attractive if the effect of temperature could be quickly evaluated. In this section, the previous lower bound shakedown approach of Wang and Yu (2013b) was extended to address this point by introducing two empirical equations related to stiffness modulus and cohesion of asphalt mixtures. The first empirical equation was given in the UK Highways Agency Design Manual (Highways agency 2006), which defined the relationship between stiffness modulus and temperature. By using this equation, the stiffness moduli (E_T) of an asphalt mixture at any temperature (T) can be estimated according to a given stiffness modulus ($E_{T'}$) at a certain temperature (T') (Eq. 4). This

empirical equation is called the HA equation and has been compared with a number of experimental data (Thom 2008). The second empirical equation (Eq. 5) is proposed by the authors based on the results from a variety of tests (Fwa et al. 2004; Wang et al. 2008; Li et al. 2011; Kim et al. 2017) as shown in Figure 14. By using Eq. 5, the cohesion ($c_{T'}$) at any temperature (T') can be predicted according to the cohesion of an asphalt mixture (c_T) at a certain temperature (T) which is recommended to be no less than 40°C. An example representing Eq. 5 is shown in Figure 14 (the red curve), which considers the asphalt mixture used in the current study (i.e. c_T = 315.1 kPa at 40°C). Note that the friction angle of an asphalt mixture mainly depends on its aggregate skeleton rather than the binder properties, and therefore the temperature has a negligible effect on the friction angle (Goetz 1989, Tan et al. 1994, Wang 2015). Finally, a temperature-dependent shakedown approach is established based on the Eq. 2-5. It should be noticed that the shakedown approach is most applicable for those asphalt mixtures in which the aggregate skeleton takes most of the stresses.

$$\log_{10}(E_T) = -0.0003[(20-T)^2 - (20-T')^2] + 0.022(T'-T) + \log_{10}(E_{T'}) \quad (4)$$

$$c_T = -745.3 \times (\ln(T) - \ln(T')) + c_{T'} \quad (5)$$

Influence of temperature on the shakedown limit of the experimental case

Based on the test data at 40°C, the stiffness and cohesion of the asphalt mixture and thereby the shakedown limit of the experiment pavement system can be obtained at different temperatures. Figure 15 shows the variation of the shakedown limit for Case 6 in Table 3 considering a range of temperatures from 20°C to 60°C. It demonstrates that increasing temperature leads to reducing the shakedown limit. The critical layer is the asphaltic layer. The pavement will lose its strength against any repeated moving wheel load at a pavement temperature of around 60°C.

Influence of temperature on the shakedown limit of a typical asphalt pavement

Further studies were conducted considering a typical three-layer asphalt pavement in TRRL Report LR1132 (Powell et al. 1984). In the report, the wheel load was assumed to be distributed uniformly in a circular contact area with a radius of 0.151m, and the elastic parameters (E, υ) of the materials at a design temperature of 20°C were also provided, as exhibited in Table 4. In order to perform shakedown analysis, typical strength parameters (c, ϕ) were also selected considering the test results in previous research (e.g. Kulhawy and Mayne 1990, MnDOT 2007, Fwa 2004, Wang 2015). Based on these parameters, the stiffness moduli and cohesion of the asphalt mixture at various temperatures were calculated by Eqs.4-5, as presented in Figure 16. The elastic stress fields were obtained by using a 3D model with a circular contact area, similar to that in Wang and Yu (2013b). Figure 17 demonstrates the change of the shakedown limit of each layer with the temperature when h_1 = 300 mm and h_2 = 450 mm. It can be seen that the shakedown limit of each layer always decreases with increasing temperature. Moreover, the reduction is more pronounced for the asphaltic layer than the granular layer. Therefore, the asphalt layer failure becomes the main failure mode when the temperature is high.

Influence of layer thicknesses at a high temperature

Hofstra and Klopm (1972) indicated that the temperature of the pavement surface can reach as high as 60°C in the UK. Considering this high temperature, the variation of the shakedown limit with the thicknesses of the first and second layers for the typical asphalt pavement is plotted in Figure 18, which demonstrates that when the layer combination is on the left-hand side of the red line, the pavement failure is controlled by the stresses in the second layer; whereas on the right-hand side, pavement failure initiates in the first layer instead. It also demonstrates that when failure occurs in the first layer, increasing

the layer thicknesses barely changes the shakedown limit. Further studies (Figure 19) show that, under such a high temperature, though the increase of layer thicknesses can significantly raise the shakedown limits of the second and third layers, its influence on the first layer shakedown limit is minor; and the first layer shakedown limit gradually converges to a constant value with increasing thicknesses. Therefore, solely changing the layer thicknesses is not an efficient and economical way of improving the pavement stability against rutting. Instead, efforts should be made to improve the shear strength properties of the asphalt mixtures at high temperatures.

Conclusions

In the present study, an experimental shakedown limit range was obtained for a layered asphalt pavement system using wheel tracking tests at a temperature of 40°C. The friction angles, cohesion and stiffness of the asphalt mixture and the crushed granite were obtained through a series of laboratory tests and then used as input values for the theoretical shakedown analysis. This was developed based on the assumption that the asphalt mixtures have a very good aggregate skeleton and the viscous properties of bitumen barely contribute to the final permanent deformation in the mixture.It was found that the theoretical shakedown limits broadly agree with the experimental result.

A relation between the cohesion of asphalt mixture and the pavement temperature was also proposed in this study. This relation, as well as the HA equation for asphalt stiffness, was introduced in the shakedown analysis of asphalt pavements, and a temperature-dependent shakedown approach was thus developed. Early indications are that this approach will be able to discriminate between rut-susceptible and non-rut-susceptible constructions. By using this approach, pavement rutting failure under any required temperature could be evaluated in a convenient and rapid manner.

It was found that for a typical asphalt pavement, the shakedown limits of all layers decrease with increasing temperature. The asphalt layer failure becomes the main failure mode when the temperature is high. It was also revealed that, to improve the pavement stability against excessive rutting, a sound choice is to improve the properties of the asphaltic material at the average maximum temperature for a pavement rather than solely increasing the layer thicknesses.

References

Alnedawi, A., Nepal, K. P. and Al-Ameri, R., 2019. New shakedown criterion and permanent deformation properties of unbound granular materials. *Journal of Modern Transportation*, 27(2), 108-119.

Allou, F., Petit, C., Chazallon, C., and Hornych, P., 2010. Shakedown approaches to rut depth prediction in low-volume roads. *Journal of Engineering Mechanics*, 136(11), 1422-1434.

Ahmad, J., Rahman, M. A. and Hainin, M. R., 2011. Rutting evaluation of dense graded hot mix asphalt mixture. *International Journal of Engineering and Technology,* 11, 56-60.

Bai, F., Yang, X. and Zeng, G., 2014. Creep and recovery behavior characterization of asphalt mixture in compression. *Construction and Building Materials*, 54, 504-511.

Boulbibane, M., Collins, I., Weichert, D. and Raad, L., 2000. Shakedown analysis of anisotropic asphalt concrete pavements with clay subgrade. *Canadian geotechnical journal,* 37**,** 882-889.

Boulbibane, M. and Ponter, A. R. S., 2005, Linear matching method for limit load problems using the Drucker-Prager yield condition. *Géotechnique,* 55, 731-739.

Brett, J. F., 1987. Stability and shakedown in pavement roughness change with age. *New Zealand Roading Symposium*, Wellington, New Zealand ,4, 695-704.

British standard Institution, 2001. BS 12697-28: 2001. *Bituminous mixtures. Test methods for hot mix asphalt-Preparation of samples for determining binder content, water content and grading*.

Brown, S. F., Yu, H. S., Juspi, S. and Wang, J., 2012. Validation experiments for lower-bound shakedown theory applied to layered pavement systems. *Géotechnique*, 62(10), 923-932.

Chazallon, C., Koval, G., Hornych, P., Allou, F., and Mouhoubi, S., 2009. Modelling of rutting of two flexible pavements with the shakedown theory and the finite element method. *Computers and Geotechnics*, 36(5), 798-809.

Chen, H. and Ponter, A. R., 2005. The linear matching method for shakedown and limit analyses applied to rolling and sliding point contact problems. *Road Materials and Pavement Design,* 6, 9-30.

Chen, Z., Yang, J. and Zhu, H., 2009. Evaluation on the shear performance of asphalt mixture through triaxial shear test. In: *Advanced Testing and Characterization of Bituminous Materials,* CRC Press, 591-600.

Chen, M., Zheng, J., Li, F., Wu, S., Lin, J., and Wan, L., 2015. Thermal performances of asphalt mixtures using recycled tyre rubber as mineral filler. *Road Materials and Pavement Design*, 16(2), 379-391.

Collins, I. F. and Cliffe, P. F., 1987. Shakedown in frictional materials under moving surface loads. *International Journal for Numerical and Analytical Methods in Geomechanics,* 11, 409-420.

Dawson, A. R. Wellner, F., 1999. *Plastic behavior of granular materials.* Final Report ARC Project 933, Reference PRG99014. University of Nottingham, UK.

European Committee for Standardization, 2004. EN 13286-7:8 2004. *Unbound and hydraulically bound mixtures - Part 7: Cyclic load triaxial test for unbound mixtures.*

Fwa, T., Tan, S. and Zhu, L., 2004. Rutting prediction of asphalt pavement layer using C-ϕ model. *Journal of Transportation Engineering,* 130, 675-683.

Goetz, W., 1989. *The evolution of asphalt concrete mix design.* Asphalt concrete mix design: development of more rational approaches, STP 1041-5-14, American society for testing and materials, Philadelphia, USA.

Highway Agency, 2006. *Design manual for roads and bridge*. London: Stationery.

Hofstra, A. and Klopm, A., 1972. Permanent deformation of flexible pavements under simulated road traffic conditions. In: *Third International Conference on the Structural Design of Asphalt Pavements,* 11-15 September 1972, London, England,1.

Juspi, S., 2007. *Experimental validation of the shakedown concept for pavement analysis and design*. Thesis (PhD). The University of Nottingham.

Kim, W. J., Lee, H. J. and Phan, H. T., 2017. Calibration and validation of a rutting model based on shear stress to strength ratio for asphalt pavements. *Construction and Building Materials,* 149, 327-337.

Kohata, Y., Tatsuokaj, F., Wang, L., Jiang, G. L., Hoque, E., and Kodaka, T.,1997. Modelling the non-linear deformation properties of stiff geomaterials. *Geotechnique*, 47(3), 563-580

Koiter, W. T. 1960. General Theorems for Elastic-Plastic Solids. In: *Progress in Solid Mechanics*, 167-221, Amsterdam.

Kootstra, B., Ebrahimi, A., Edil, T. and Benson, C., 2010. Plastic deformation of recycled base materials. In: *GeoFlorida 2010: Advances in Analysis, Modeling and* Design, 2682-2691, Florida, USA.

Krabbenhøft, K., Lyamin, A. V. and Sloan, S. W., 2007. Bounds to Shakedown Loads for a Class of Deviatoric Plasticity Models. *Computational Mechanics,* 39, 879-888.

Kulhawy, F. H., and Mayne, P. W., 1990. *Manual on estimating soil properties for foundation design* (No. EPRI-EL-6800). Geotechnical Engineering Group.

Lambe, T. W., and Whitman, R. V., 2008. *Soil mechanics*. John Wiley & Sons, San Francisco, USA.

Lekarp, F., Richardson, I. R., and Dawson, A., 1996. Influences on permanent deformation behavior of unbound granular materials. *Transportation research record*, 1547(1), 68-75.

Li, P., Jiang, X., Guo, K., Xue, Y., and Dong, H. 2018. Analysis of viscoelastic response and creep deformation mechanism of asphalt mixture. *Construction and Building Materials*, 171, 22-32.

Li, Q., Lee, H. J. and Lee, S. Y., 2011. Permanent deformation model based on shear properties of asphalt mixtures: Development and calibration. *Transportation Research Record,* 2210, 81-89.

Liu, S., Wang, J., Yu, H. S. and Dariusz W., 2016. Shakedown solutions for pavements with materials following associated and non-associated plastic flow rules. *Computers and Geotechnics*, 78, 218-226.

Melan, E., 1938. Der spannungsgudstand eines Henky-Mises schen kontinuums bei verlandicher belastung. *Sitzungberichte der Ak Wissenschaften Wie (Ser. 2A)*, 147, 73.

Minnesota Department of Transportation (MnDOT). 2007. *Pavement design manual*.

Nguyen, A. D., 2007. *Lower-bound shakedown analysis of pavements by using the interior point method.* Thesis (PhD). RWTH Aachen University.

Qian, J. G., Wang, Y. G., Yin, Z. Y., and Huang, M. S., 2016. Experimental identification of plastic shakedown behavior of saturated clay subjected to traffic loading with principal stress rotation. *Engineering Geology*, 214, 29-42.

Powell, W. D., Potter, J. F., Mayhew, H. C. and Nunn, M. E., 1984. *The structural design of bituminous roads, TRRL Laboratory report 1132*, Transportation and Road Resaech laboratory, Crowthorne, Bershire, UK.

Raad, L., Weichert, D. and Najm, W., 1988. Stability of multilayer systems under repeated loads. *Transportation Research Record*,1207.

Rees, S., 2013. Introduction to triaxial testing[online]. GDS company. Available from: www.gdsinstruments.com.

Seed, H. B., Lundgren, R., 1954. Investigation of the effect of transient loading on the strength and deformation characteristics of saturated sands. In *Proceedings-American Society for Testing and Materials*, 54, 1288-1306.

Sharp, R. W., 1985. Pavement design based on shakedown analysis. *Transportation Research Record,* 1022, 107.

Sharp, R. W. and Booker, J. R., 1984. Shakedown of pavements under moving surface loads. *Journal of Transportation Engineering,* 110, 1-14.

Svoboda, J., 2014. Shearing rate effects on dense sand and compacted clay. *Dynamic Behavior of Materials*, 1*,* 389-395.

Tan, S. A., Low, B. H. and Fwa, T., 1994. Behavior of asphalt concrete mixtures in triaxial compression. *Journal of Testing and Evaluation,* 22, 195-203.

Thom, N., 2008. *Principles of pavement and engineering*. London: Thomas Telford Publishing.

Wang, H. N., Liu, X. J. and Hao, P. W., 2008. Evaluating the shear resistance of hot mix asphalt by the direct shear test. *Journal of Testing and Evaluation,* 36, 485-491.

Wang, J. G., 2015. *Characterization of failure and permanent deformation behaviour of asphalt concrete*, Thesis (PhD). Delft University of Technology.

Wang, J., Liu, S., and Yang, W., 2018. Dynamics shakedown analysis of slab track substructures with reference to critical speed. *Soil Dynamics and Earthquake Engineering*, 106, 1-13.

Wang, J., Liu, S. and Yu, H.S., 2018. Recent Progress on Lower-Bound Shakedown Analysis of Road Pavements. In *Advances in Direct Methods for Materials and Structures (129-142)*. Springer, Cham.

Wang, J. and Yu, H. S., 2014. Three-dimensional shakedown solutions for anisotropic cohesive-frictional materials under moving surface loads. *International Journal for Numerical and Analytical Methods in Geomechanics,* 38, 331-348.

Wang, J. and Yu, H.S., 2013a. Residual stresses and shakedown in cohesive-frictional half-space under moving surface loads. *Geomechanics and Geoengineering*, 8(1), 1-14.

Wang, J. and Yu, H. S., 2013b. Shakedown analysis for design of flexible pavements under moving loads. *Road Materials and Pavement Design*, 14(3), 703-722.

Wasage, T., Statsna, J. and Zanzotto, L., 2010. Repeated loading and unloading tests of asphalt binders and mixes. *Road Materials and Pavement Design,* 11, 725-744.

Wellner, F., Werkmeister, S., 2000. Beitrag zur Untersuchung des Verformungsverhaltens ungebundener Gesteinskörnungen mit Hilfe der Shakedown-theorie. *Straße und Autobahn*, 51(6), 369-375.

Werkmeister, S., Dawson, A. R. and Wellner, F., 2005. Permanent Deformation Behaviour of Granular Materials. *Road Materials and Pavement Design*, 6 (1), 31-51.

Yu, H. S., 2006. *Plasticity and geotechnics*. Springer Science & Business Media.

Yu, H. S. and Wang, J., 2012. Three-dimensional shakedown solutions for cohesive-frictional materials under moving surface loads. *International Journal of Solids and Structures,* 49, 3797-3807.

Zhao, J., Sloan, S. W., Lyamin, A. V. and Krabbenhøft, K., 2008. Bounds for shakedown of cohesive-frictional materials under moving surface loads. *International Journal of Solids and Structures,* 45, 3290-3312.

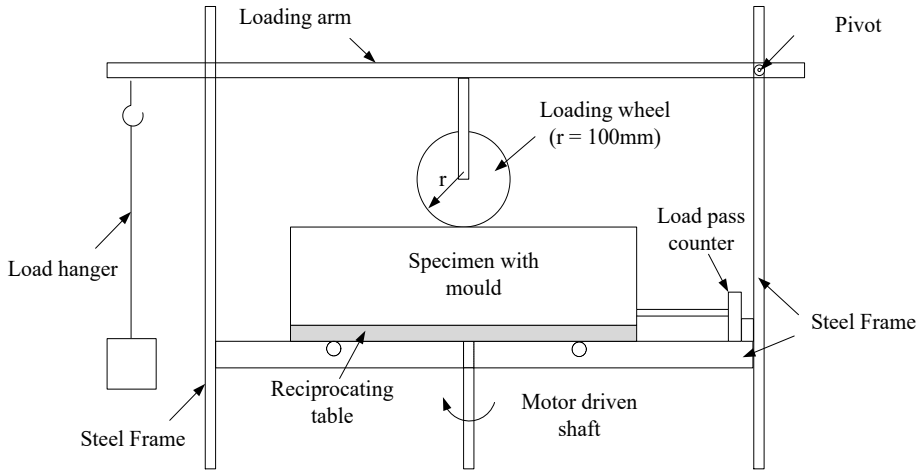

Figure 1. Schematic of Wheel Tracking Equipment

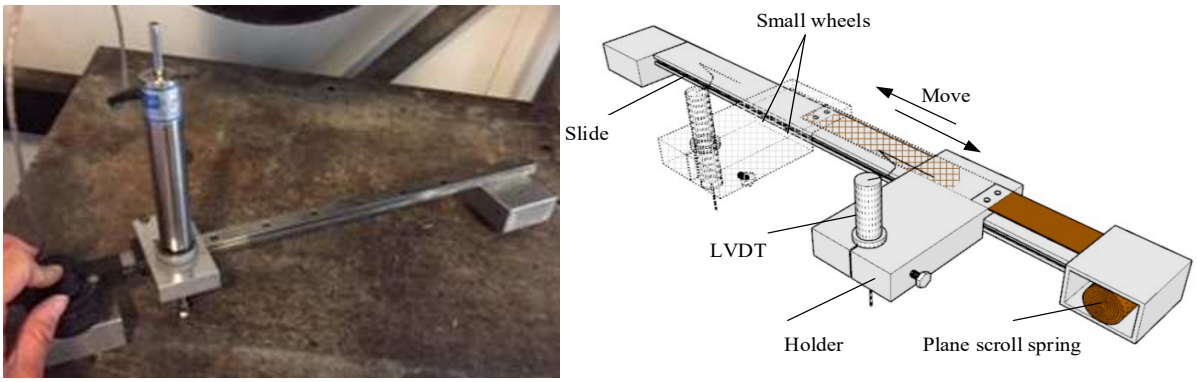

Figure 2 LVDT and movable holder

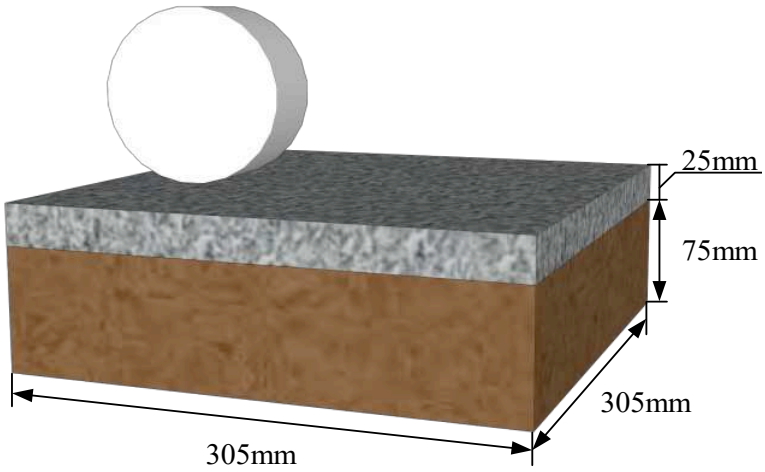

Figure 3 Sketch of the two-layered asphalt pavement system

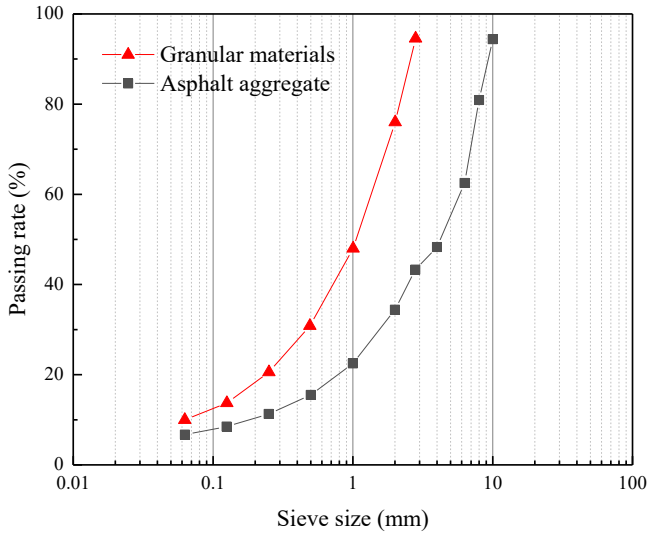

Figure 4 Grading curves of granular materials and aggregates in the asphalt mixture

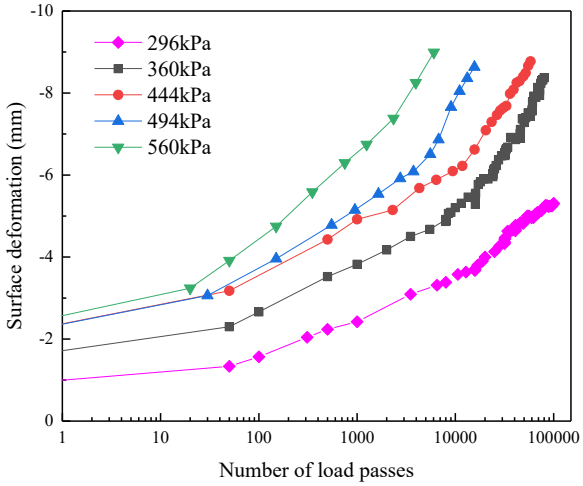

Figure 5 Development of rutting depth under different magnitudes of load

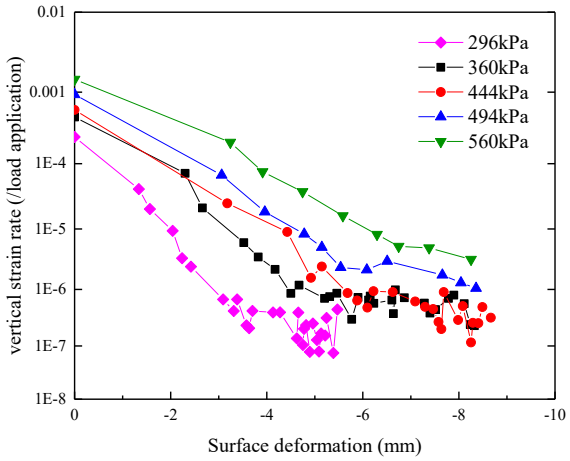

Figure 6 Change of vertical strain rate against surface deformation

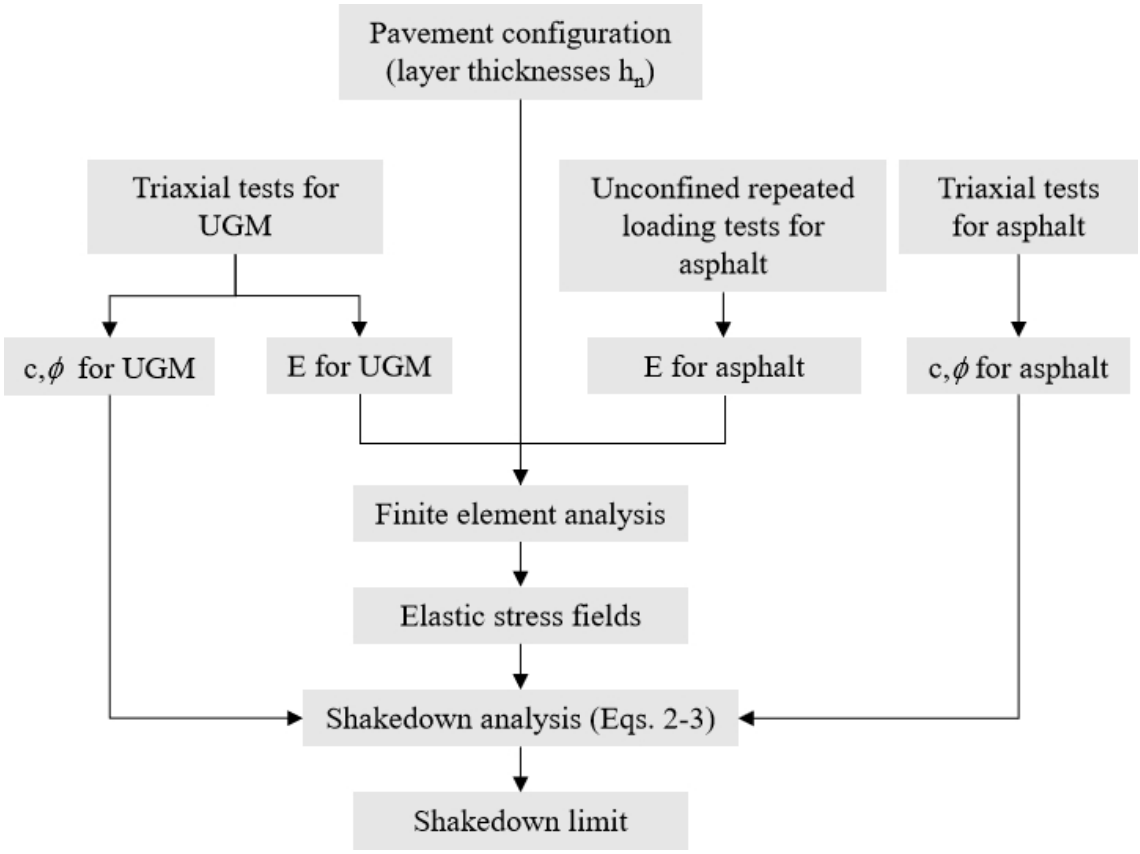

Figure 7 Flow chat of the experiment methodology

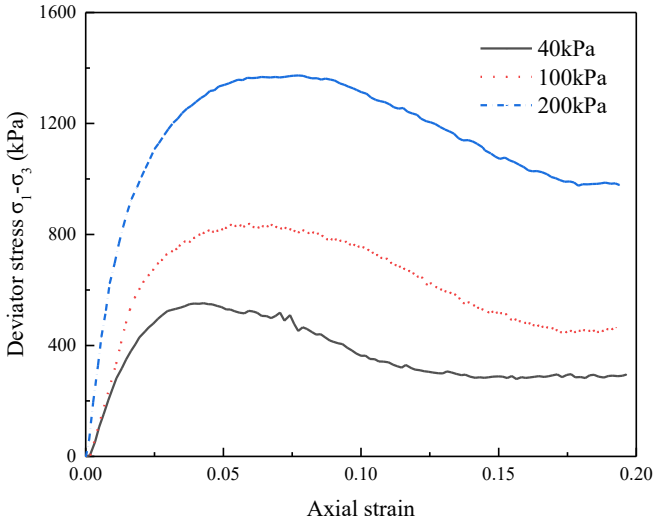

(a) Dry specimen

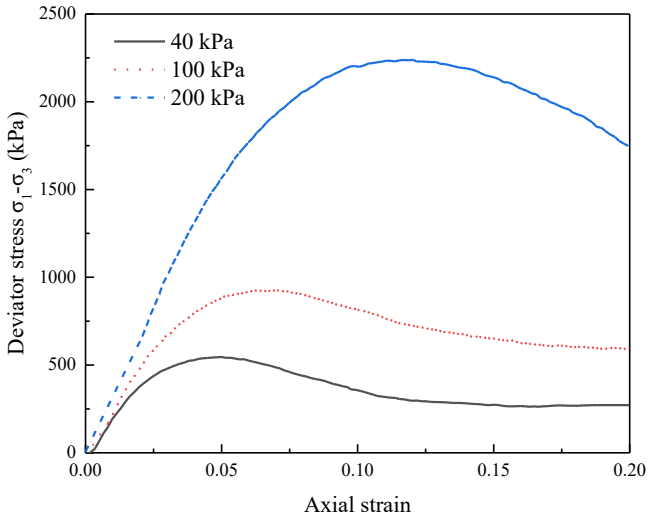

(b) Saturated specimen

Figure 8 Stress - strain responses under different confining pressures

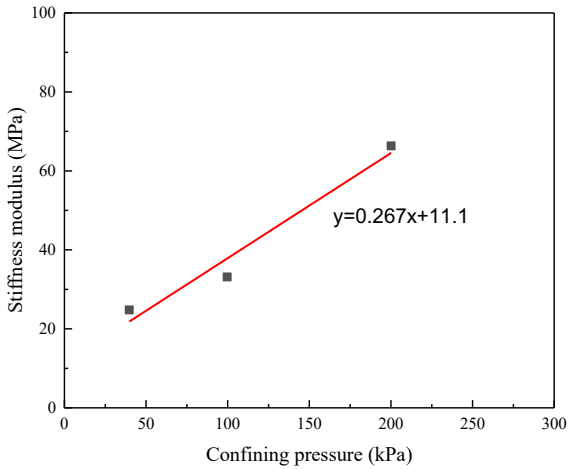

(a) Dry specimen

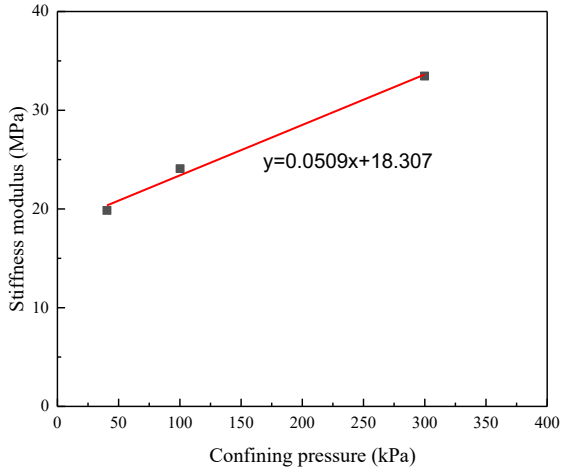

(b) Saturated specimen

Figure 9 Stiffness moduli against confining pressures for the crushed granite

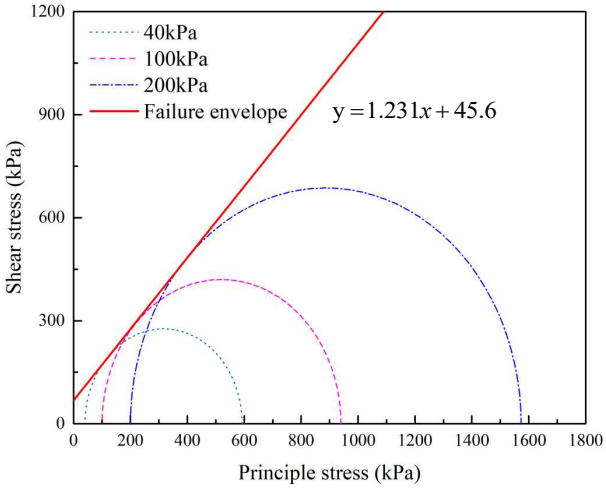

(a) Dry specimen

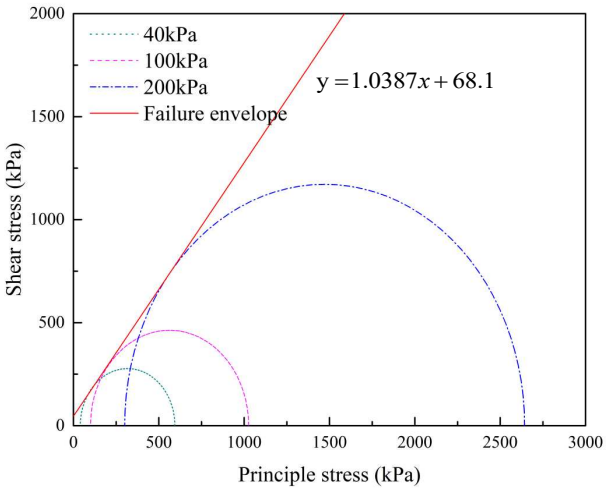

(b) Saturated specimen

Figure 10 Mohr circles and failure lines of the crushed granite

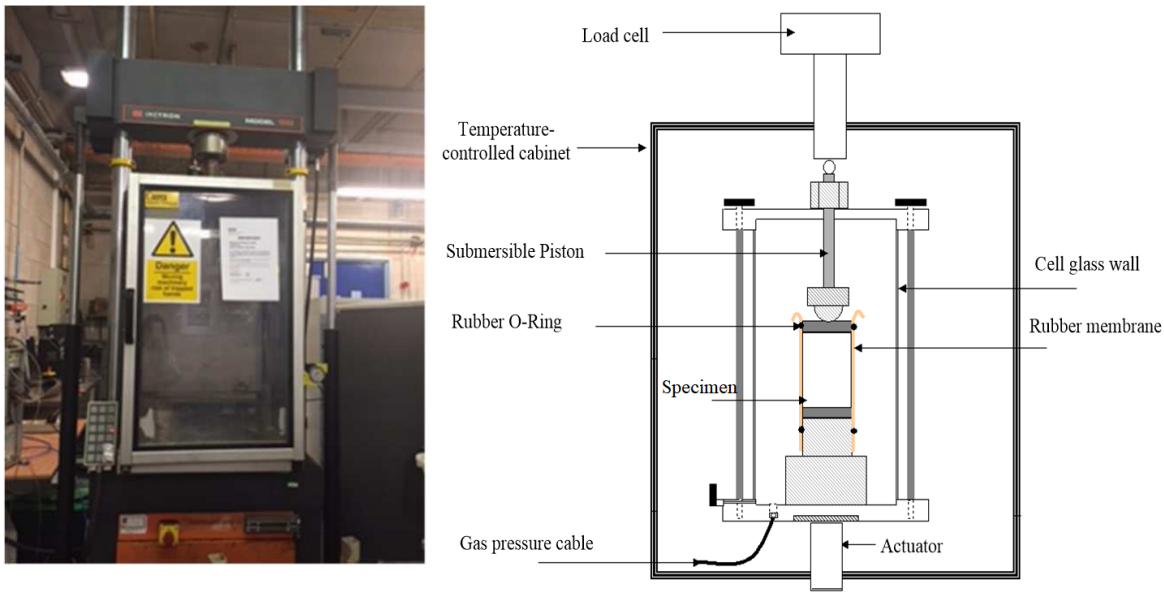

Figure 11 Instron Universal Testing Machine (UTM) at the University of Nottingham

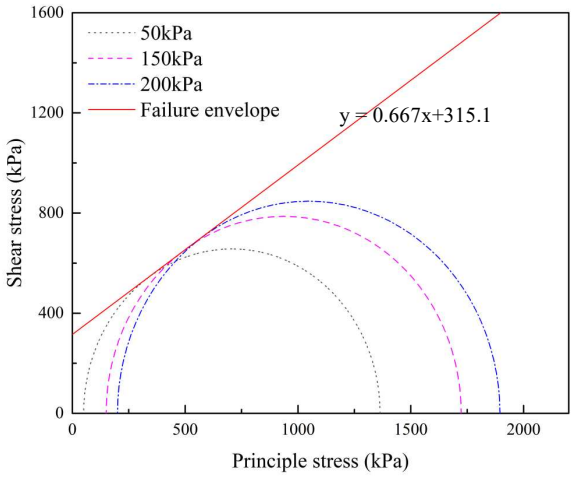

Figure 12 Mohr circles and failure line of the asphalt mixture

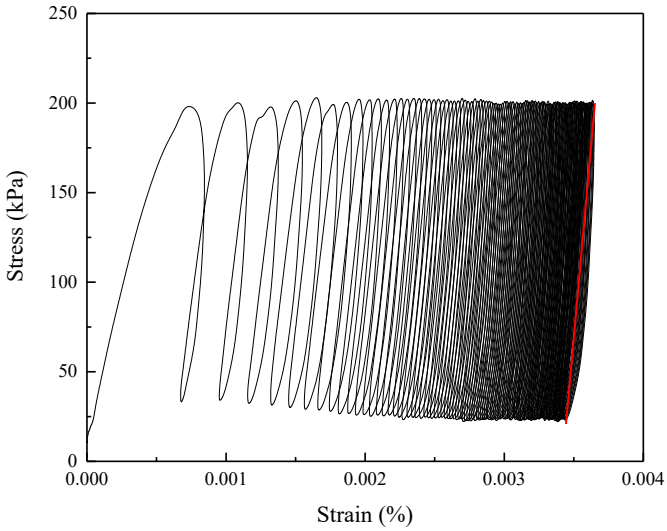

Figure 13 Cyclic stress-strain response of the asphalt mixture

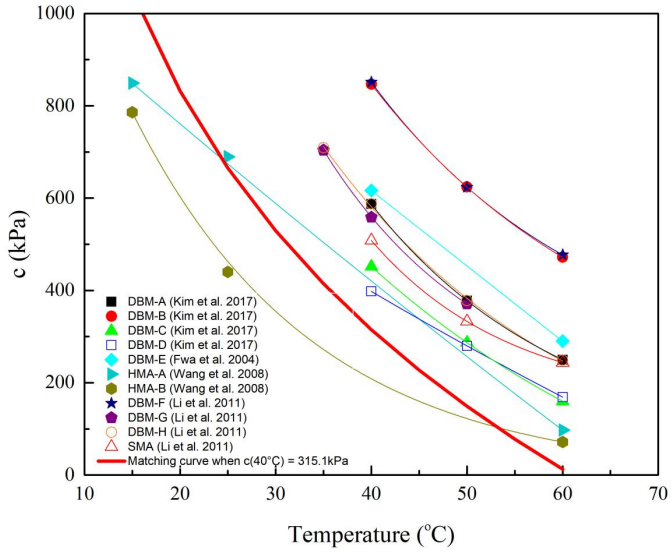

Figure 14 Change of the cohesion of different asphalt mixtures with temperature 40°C

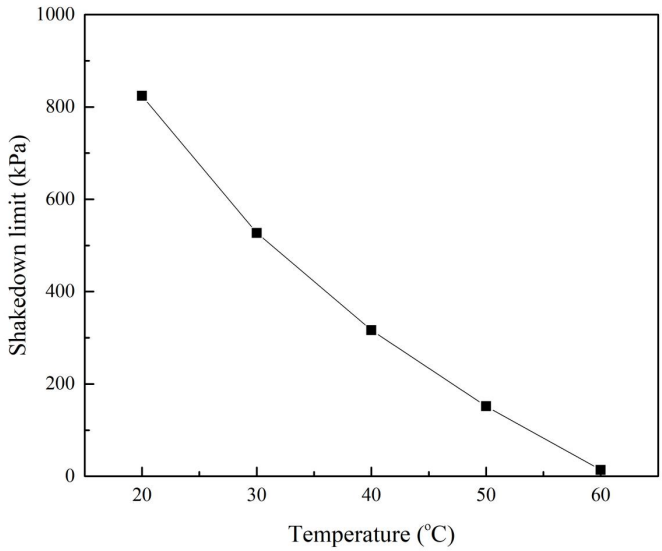

Figure 15 Effect of temperature on the shakedown limit of the experimental case

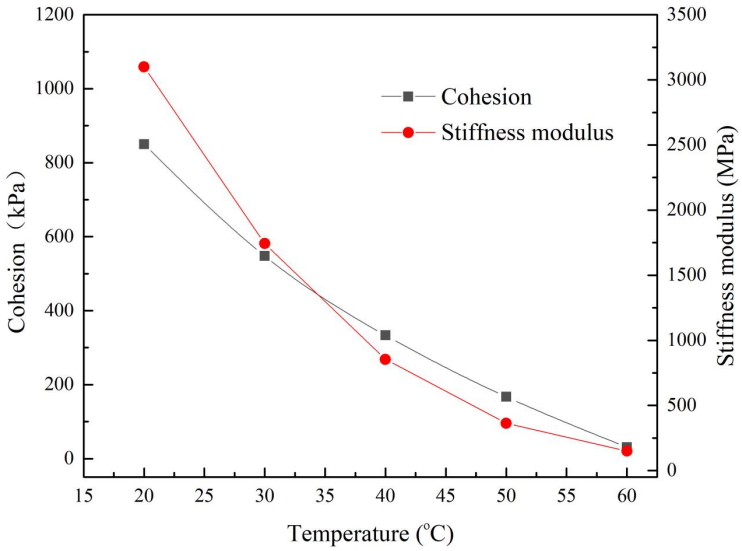

Figure 16 Elastic modulus and cohesion of the DBM at different temperatures

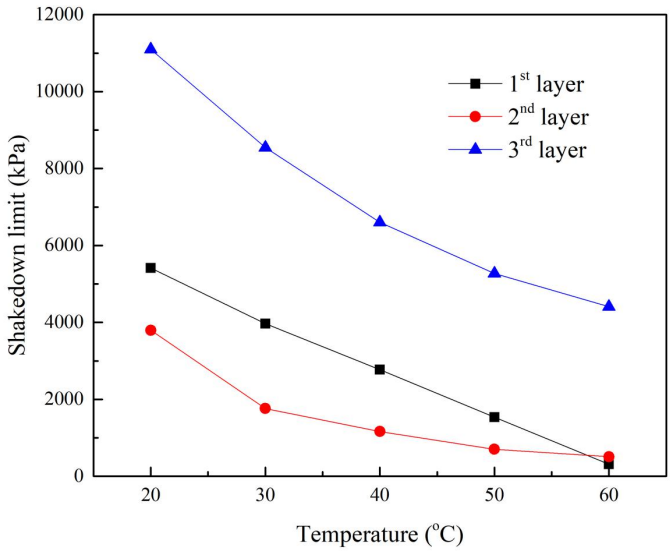

(a) $\mu = 0$

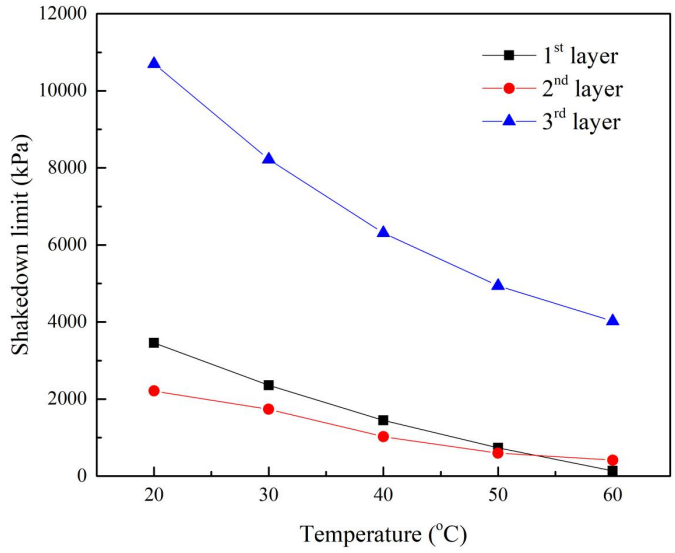

(b) $\mu = 0.3$

Figure 17 Effect of temperature on the shakedown limit of each layer (h_1 = 300mm, h_2 = 450mm)

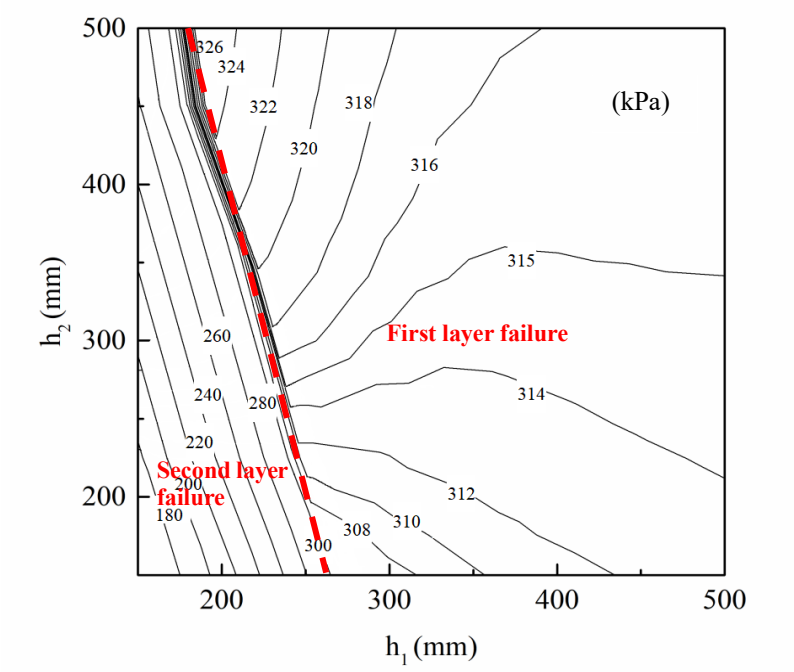

Figure 18 Counter plot of shakedown limits for an asphalt pavement at 60˚C and $\mu = 0$

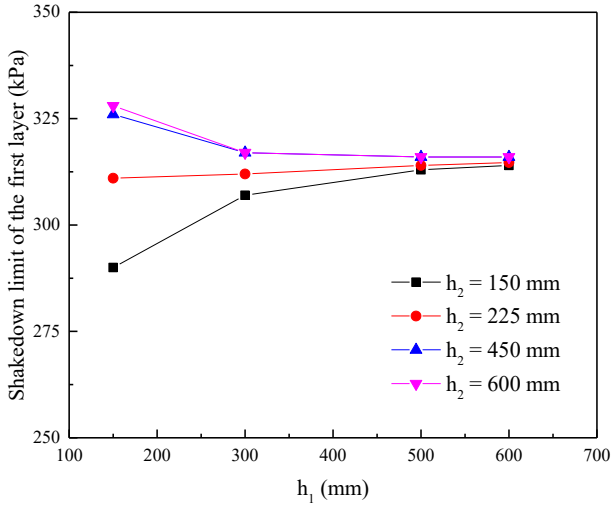

(a) First layer

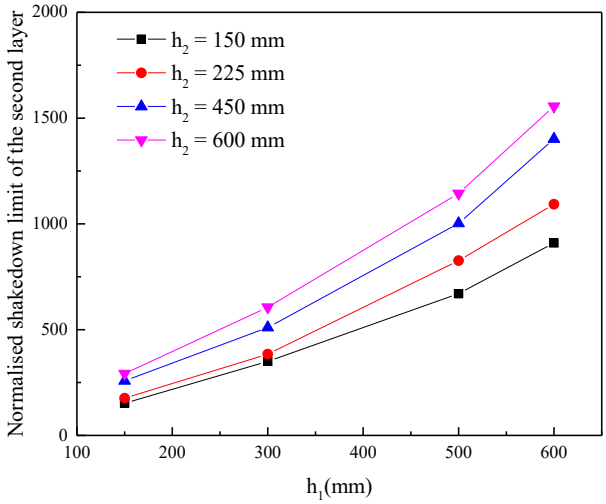

(b) Second layer

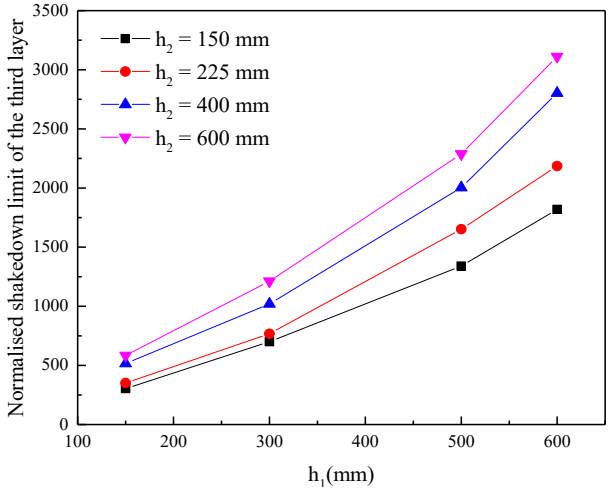

(c) Third layer

Figure 19 Effect of layer thicknesses on the shakedown limit of each layer at 60˚C and $\mu = 0$

Table 1. Calculations of the contact pressure under different magnitudes of load

	Test 1	Test 2	Test 3	Test 4	Test 5
Load applied (N)	473.3	606.6	807.0	941.4	1139.5
Length of contact area $2a$ (m)	0.0320	0.0337	0.0364	0.0381	0.0407
Width of contact area (m)	0.05	0.05	0.05	0.05	0.05
Contact pressure (kPa)	296	360	443	494	560

Table 2 Materials properties

Materials	Stiffness modulus E (MPa)	Cohesion c (kN)	Friction angle ϕ (°)
Asphalt (at 40°C)	891.8	315.1	34.1
Crushed granite (dry)	18.3	45.6	50.9
Crushed granite (saturated)	11.1	46.1	68.1

Table 3 Theoretical shakedown solutions for the wheel tracking cases

Case	E_1 (MPa)	c_1 (kPa)	ϕ_1 (°)	υ_1	E_2 (MPa)	c_2 (kPa)	ϕ_2 (°)	υ_2	μ	shakedown limit (kPa)
1	891.8	315.1	34.1	0.3	18.3	45.6	50.9	0.3	0	676.4
2	891.8	315.1	34.1	0.3	18.3	45.6	50.9	0.3	0.3	663.3
3	891.8	315.1	34.1	0.3	18.3	45.6	50.9	0.3	1	319.3
4	891.8	315.1	34.1	0.3	11.1	68.1	46.4	0.3	0	601.1
5	891.8	315.1	34.1	0.3	11.1	68.1	46.4	0.3	0.3	591.1
6	891.8	315.1	34.1	0.3	11.1	68.1	46.4	0.3	1	316.6

Table 4 Properties of a flexible pavement structure at 20˚C

Layer	Type	h_n (mm)	E_n (MPa)	c_n (kPa)	υ_n	ϕ_n (°)
1	DBM	150~600	3100	850	0.35	40
2	Granular material	150~600	150	10	0.3	44
3	Subgrade soil	∞	50	20	0.45	18

Note: the subscript *n* represents layer number.